Measuring podded propeller performance in ice

Akinturk, A.; Jones, S. J.; Rowell, B.; Duffy, D.

1st International Conference on Technological Advances in Podded Propulsion [Proceedings], 2004

IR-2004-01

MEASURING PODDED PROPELLER PREFORMANCE IN ICE

A. Akinturk, National Research Council (NRC), Institute for Ocean Technology (IOT), Canada
S. J. Jones, NRC – IOT, Canada
B. Rowell, NRC – IOT, Canada
D. Duffy, NRC – IOT, Canada

Ever since their first appearances, azimuthing podded propulsors have become increasingly popular. In a parallel development, there has been an increasing interest in arctic shipping. Hence, the number of vessels with azimuthing podded propulsors being capable of navigating in arctic conditions is increasing. The aim of this study is to help the understanding of ice effects on this type of propulsors. The knowledge generated could then be used in updating the regulations governing the design of vessels for arctic navigation, including the podded propulsion systems, by the International Association of Classification Societies.

The paper describes the preliminary experimental results obtained in this study so far. The setup designed and built at NRC-IOT, Canada, has the capability of measuring the loads on a podded propeller system operating in ice. It is able to measure loads on the entire model, propeller shaft bearing loads and blade loads. The results suggested that the bearings undergo cyclic loading conditions during the encounters with ice.

1. Introduction

Increasingly, maritime activities are being conducted in harsh environments. The offshore oil and gas industry is accelerating on the Canadian East Coast and is expected to open up the West Coast and Arctic regions in the next few years. As the increased interest in arctic shipping continues, new constructions designed to include ice navigation as a part of their expected working year, are adapting different propulsion systems based on their open water characteristics for use in ice. These systems include podded propulsors, whose ability to direct thrust in any direction greatly improves maneuverability.

Podded propulsors were introduced to the marine industry around mid nineties. They have become popular in the last few years or so. They have continued to grow in size and power. The power ranges reported in the literature varies considerably: from 1530kW [1], [2] to 30000kW [3]. The rapid adoption of podded drives by the marine industry has outpaced the understanding of their performance. The lack of knowledge has translated into difficulties in practice, such as propeller and bearing damage and extreme vibration during manoeuvering.

A podded propulsion system is a unit in which either a motor to drive the propeller is placed inside the pod or alternatively mechanically geared with motor outside the pod. The pod and the propeller are mounted to the ship hull through a strut. The whole unit can rotate. This rotation, or azimuthing capability, allows the thrust developed by the propellers to be directed anywhere within a 360° compass. This eliminates the need for rudders and provides extremely favorable maneuverability characteristics to the vessel. They have different operational configurations: pull (tractor) or pusher mode.

The loads on podded propulsors for arctic shipping are generally taken as loads on open propellers and they do not include the loads on the whole unit themselves. Hence, this study aims to increase the understanding of the performance of podded propulsors in ice. A set of experiments has been

designed to measure the contact ice loads on a model podded propulsion system. The objective of these tests is to determine a relationship between the ice thickness, in which a vessel navigates, and the resulting cyclic loading experienced by the pod, stern bearing and propeller. This relationship would then be used to modify existing shipping regulations pertaining to the machinery design for arctic conditions.

2. Experimental Model

An experimental model has been designed and built at NRC-IOT (Fig. 1). It consists of a propeller, a pod, a strut and a model stern. The propeller, a similar design to an R-Class vessel's propeller, is 0.30m in diameter and has four blades. The pod unit with a cylindrical cross section is 0.95m long and has 0.17m diameter. The strut has a uniform cross section with a span of 0.45m. The model stern houses the dynamometer that measures global forces and moments acting overall podded system. Use of a complete model hull would be necessary to model the effects of hull ice interactions more accurately, however, this was not included in the current scope of the work.

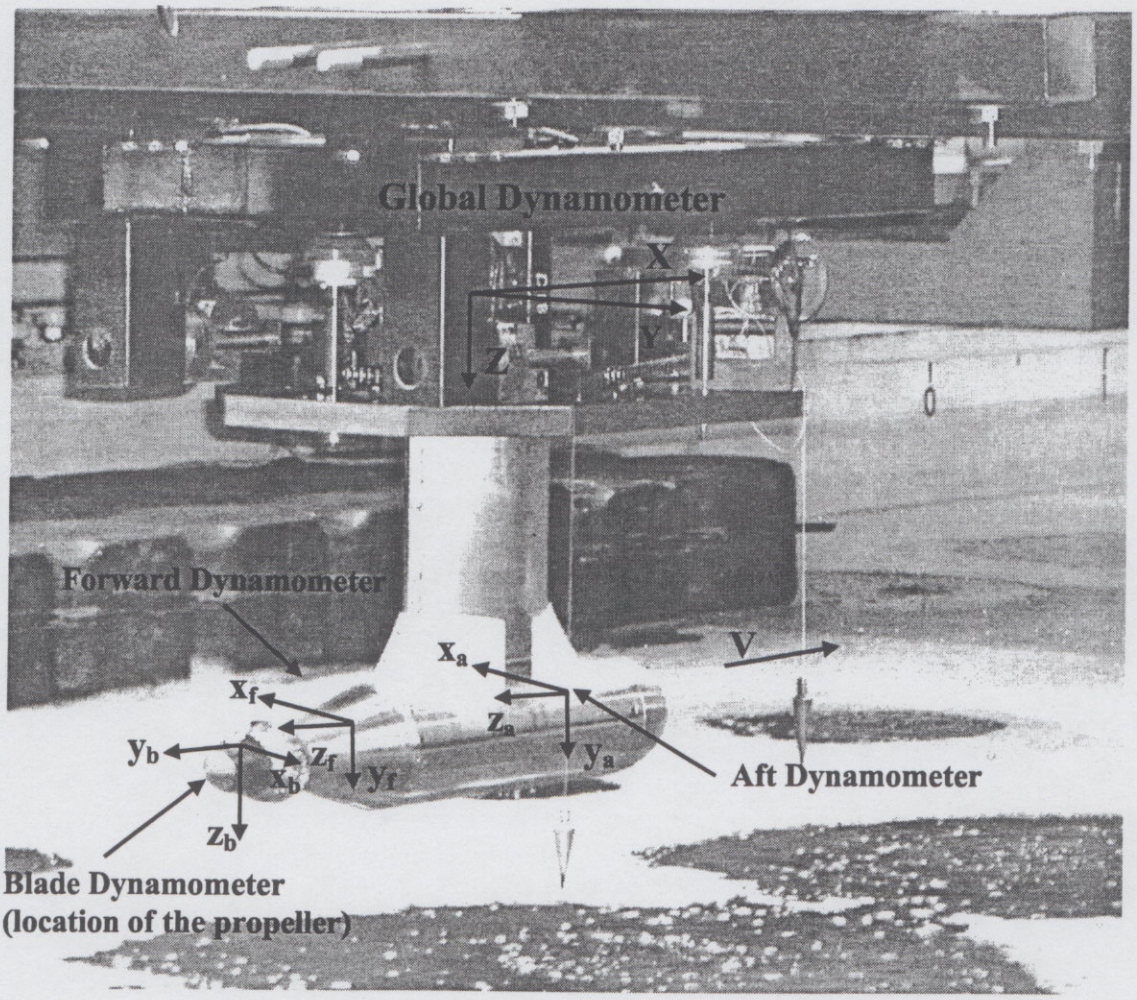

Fig. 1 - Assembled system (does not include the propeller)

There are four, six component dynamometers housed in the model. The dynamometer on the top measures global forces and moments experienced by the entire model. The remaining three dynamometers are mounted inside the pod unit. The first is attached to one of the propeller blades to record the loads on the blade. Additionally, the angular position of this blade is recorded. The two other dynamometers measure propeller shaft bearing loads. The thrust generated by the propeller

can be calculated from the outputs of these two dynamometers. A strain gauge system is used to measure propeller shaft torque near the propeller end of the shaft.

In Fig. 1, X, Y and Z denote the reference frame attached to the global dynamometer. X direction is aligned with the tank length. This reference frame is fixed to the carriage. Hence, forces in X, Y and Z directions correspond to resistance-thrust, side force and vertical force respectively. x_b, y_b, and z_b are fixed to the blade dynamometer, which is attached to one of the blades. The z axis of this dynamometer is aligned with the radial direction of the blade. This frame of reference rotates with the blade. x_f, y_f, z_f, and x_a, y_a, z_a are the reference frames attached to the forward and aft dynamometers respectively. The z-axes of these dynamometers are aligned with the propeller shaft, hence, forces measured in z_f and z_a correspond to the thrust.

2.1. Global Dynamometer

Shown in
Fig. 2 is the load cell arrangement for the global dynamometer. It consists of six high-precision 8907N load cells oriented in such a way that, it can measure the global forces and moments experienced by the entire model, the results are accurate within ± 5% of the full scale. The global dynamometer is fixed in a reference frame attached to the carriage. The strut and the pod can be rotated 360 degrees about the vertical axis using the azimuthing gear, while the model stern, hence the global dynamometer, remains fixed with respect to this frame of reference.

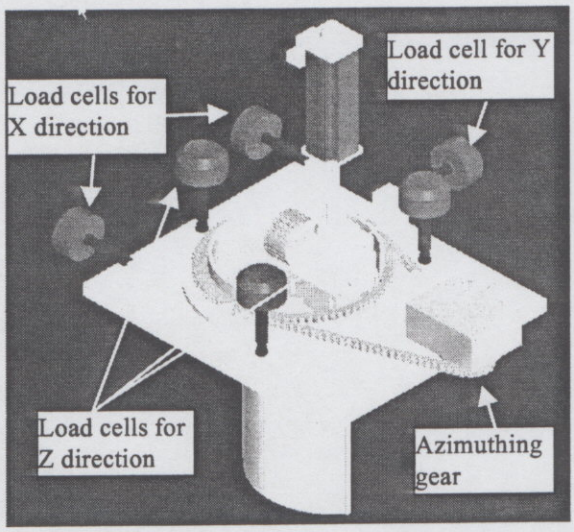

Fig. 2 - Load cell arrangements for the global dynamometer

2.2. Blade and Shaft Bearing Dynamometers

Fig. 3 shows the three dynamometers mounted inside the pod. These are identical dynamometers and capable of measuring six components: forces and moments in three orthogonal directions as shown in Fig. 1. The ratings for these dynamometers are given as follows:

- Forces in x and y directions: 2224 N
- Forces in z direction: 4448 N
- Moments in x, y and z directions: 56.5 Nm

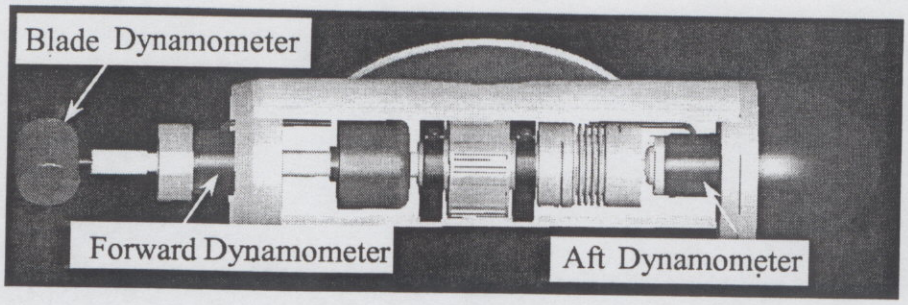

Fig. 3 - Pod and propeller assembly of the model and orientation of the six-component dynamometers

The aft dynamometer is mounted after a thrust de-coupler, therefore, is not expected to encounter as large forces or moments as the forward dynamometer.

A rotary position transducer records the angular position of the blade, to which the blade dynamometer is attached. This enables an accurate matching of the forces and moments due to the contact of the blade with ice.

The wiring for the strain gage and the blade dynamometer goes through the drive shaft and a set of slip rings to a signal conditioner. Due to the high rotational speed and the requirement of a large number of data points over each time a blade-ice contact occurs, each of these channels is sampled at 5000 Hz.

3. Ice tank

3.1. Ice Tank Facilities

The NRC-IOT ice tank is 3m deep, 76m long and 12 m wide. A set up area is separated from the ice sheet by a thermal barrier door in order to facilitate setup while the ice sheet is growing. At the opposite end of the tank is located a sloped ramp leading into a melt pit. This pit has an insulated cover allowing an ice sheet in the tank to be grown while the remains of the previous one are melting. The ice tank is equipped with a towing carriage that is capable of velocities from 0.1 to 4.0 m/s. It is designed with a central testing area where a test frame, mounted to the carriage, allows the experimental setup to move transversely across the entire width of the tank. The control room is thermally insulated and houses the computer equipment for the drive control and the instrumentation racks for the model test transducers [2].

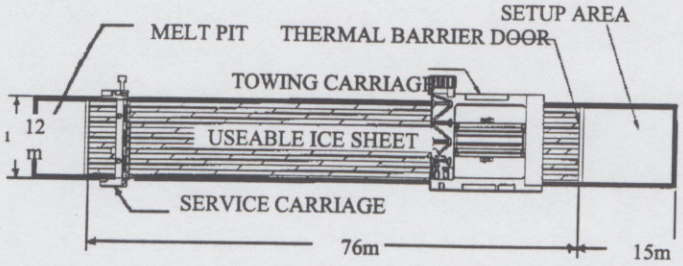

ICE TANK
3m DEEP

Fig. 4 - A schematic of the ice tank

3.2. Model Ice

For these tests model EG/AD/S ice was used. EG/AD/S ice is designed to provide the scaled flexural failure strength of real sea ice and is made up of a mixture of water, (E)thylene (G)lycol, (A)liphatic (D)etergent and (S)ugar [5]. This formulation can be improved by incorporating tiny air bubbles in the ice to correct its density to give the same buoyancy to the ice as is found at full-scale. The creation of the ice sheet begins with a seeding process and it continues to grow at a temperature of around –20°C until it reaches the target thickness. In order to obtain the target strength the ice is tempered. This involves warming the facility to a temperature of +2°C in order to soften the ice. The tempering process mentioned above causes the disintegration of model ice along the grain boundaries. Due to this, the failure behavior of the model ice is different than that of sea ice. Nevertheless, the failure envelope of EG/AD/S ice is reported to be as good as other model ices', even superior in some aspects [5].

4. Experiments

The results presented in this paper are based on the preliminary experiments. The experiments consisted of clear water and ice tests. During the experiments, two separate ice sheets were used. A total of 84 runs were conducted, 36 were in clear water and the remaining tests were in level ice conditions. During the tests the azimuthing angle, θ, was varied from 0° to 180 ° degrees in 45 ° intervals in both push and pull mode.

The target flexural strength for the tests was 60 kPa at the start of each set of experiments. The ice sheet was generated with a target thickness of 60 mm. Along the course of the experiments the ice density, thickness, flexural, compressive and shear strength values were sampled periodically.

Before the experiments, each ice sheet was cut into three longitudinal sections in order to maximize the number of tests. This prevented undesirably long propagations of cracks across the width of the ice sheet.

4.1. Flexural strength

The target flexural strength for the experiments was 60kPa, however, during the course of the experiments ice sheets thawed and their strength values decreased as shown in
Fig. 5. The figure gives the flexural strength of the ice sheets as a function of time. The first ice sheet used over two days. The flexural strength during these tests diminished considerably: around 10kPa compared to the 60kPa target strength. As can be seen in the graph the flexural strength of the ice decreased the most rapidly within the first five hours of testing. However, this process can be slowed down by lowering the air temperature in the tank.

4.2. Ice thickness

For the ice sheets used the target thickness was 60 mm. During the tests, the thickness was measured for the north, south and center sections of the sheet. For each section, the measurements were taken every two meters along the length on each side of the section.
Fig. 6 shows a sample ice thickness values along the tank. The nominal thickness for the given ice sheet was 65mm with ±5mm variations; the ice thickness stays relatively constant as time passes. For the ice sheet used on the first and the second days, the thickness varied between 60 mm and 70 mm, the ice sheet on the third day had a thickness between 59 mm and 62 mm.

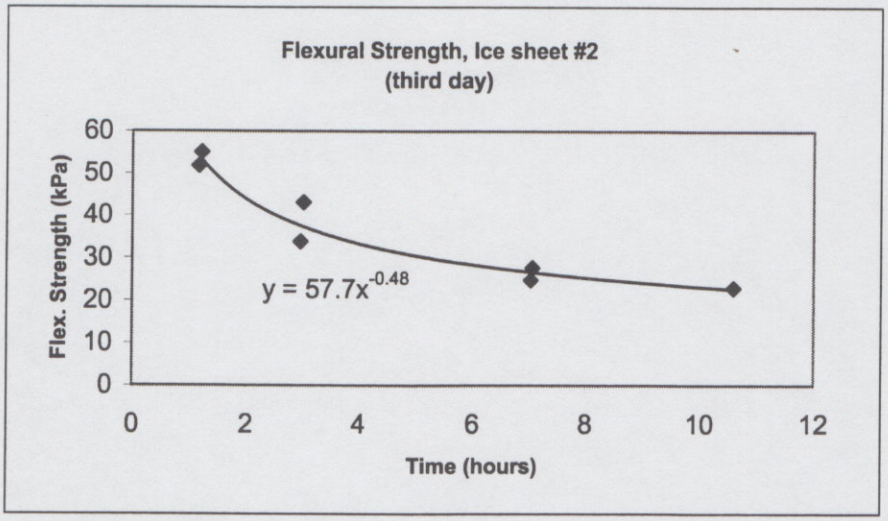

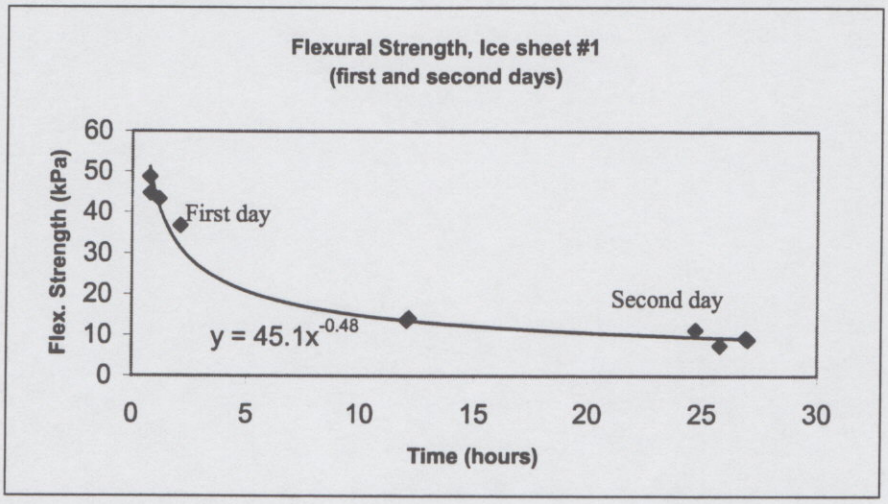

Fig. 5 - Flexural strength of the ice sheets as a function of hours since tests began.

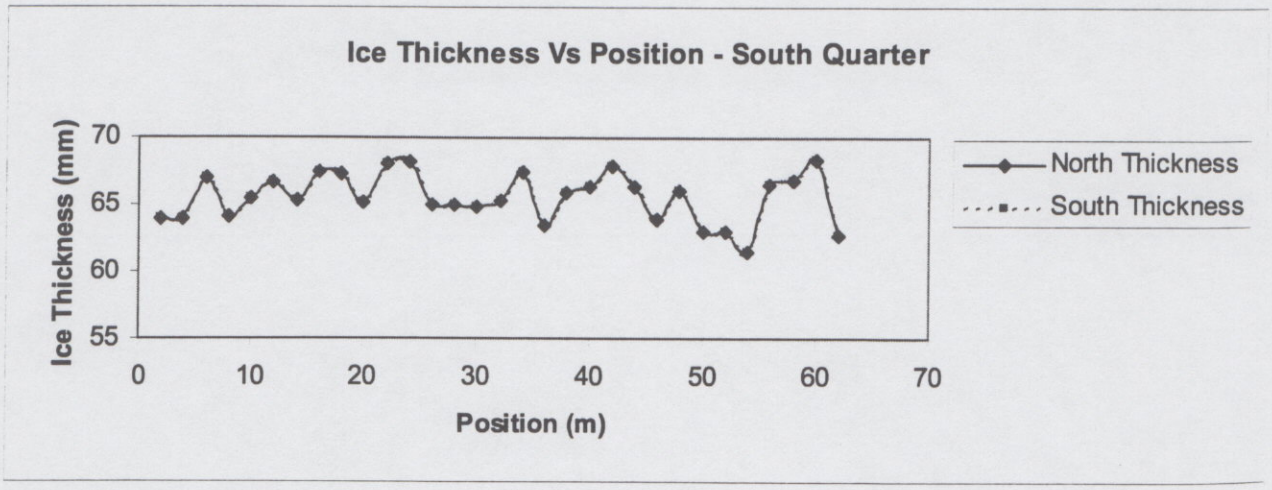

Fig. 6 - Ice thickness as a function of position

4.3. Compressive strength

On the first ice sheet, the compressive strength varied between 60kPa and 167kPa. The second ice sheet, used on the third day, shows much less variation in compressive strength. The ice sheet had an initial compressive strength of 155kPa, at the end of the experiments, its strength value dropped to 115kPa.

5. Results

5.1. In clear water

The podded propulsor model experiences different flow conditions at different operating conditions. Depending upon the forward velocity, azimuthing angle and rotational speed of the propeller, the effects of the varying flow conditions on the loads experienced can be visible in the output of the global dynamometer. Apart from the forces in X, Y and Z directions, moments in these directions can also be calculated.

Fig. 7 shows the non-dimensional global F_Y force as a function of advance coefficient (J) for clear water conditions. It is interesting to note that even at zero forward velocity while the propeller was rotating, due to the propeller induced flow conditions there was a side force acting on the model. This could perhaps be attributed to the asymmetric flow conditions generated around the strut and the pod due to propeller rotation. For this particular case, it decreased with increasing forward velocity, though, in the range considered it had still a non-zero value. This could be important to manoeuvering and directional stability of vessels outfitted with podded propulsors.

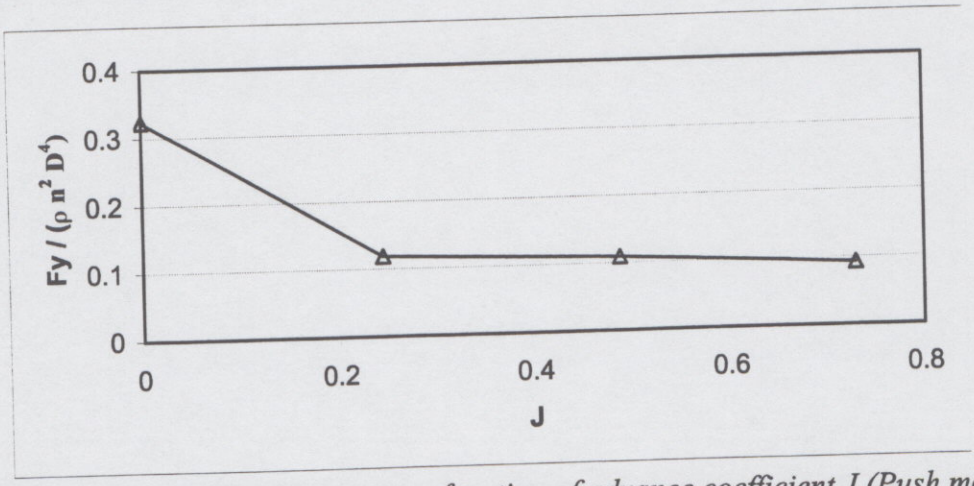

Fig. 7- Non-dimensional global F_Y force as a function of advance coefficient J (Push mode,0 degree azimuthing angle). J=0 corresponds to the case, in which propeller is rotating but forward velocity is zero in clear water conditions.

In the next figure, Fig. 8, non-dimensional global M_Y and M_Z moments are given for clear water conditions. Similarly, at J=0 (zero forward velocity and non-zero propeller rotation), M_Y and M_Z had non-zero values due to the flow generated by the propeller. As the forward velocity increased, the effects were reduced and, M_Y and M_Z decreased. The effects on M_Z seemed less pronounced compared to M_Y.

By plotting the maximum and minimum magnitudes measured during the clear water tests, Fig. 9 can be obtained. This shows the maximum and minimum forces experienced by the forward

dynamometer in x_f and y_f directions for clear water performance. As expected 90 degrees azimuthing angle had the largest forces associated with the forward dynamometer.

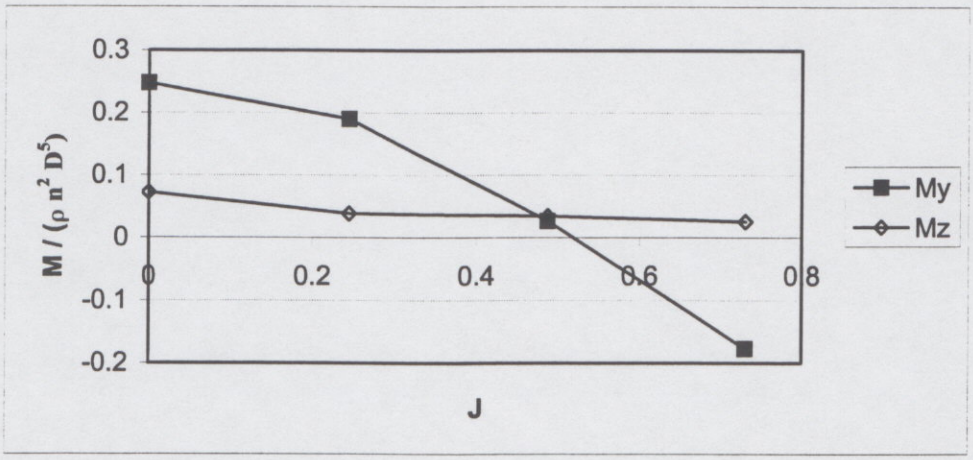

Fig. 8 - Non-dimensional M_Y and M_Z moments calculated using the global dynamometer output (Push mode,0 degree azimuthing angle, clear water)

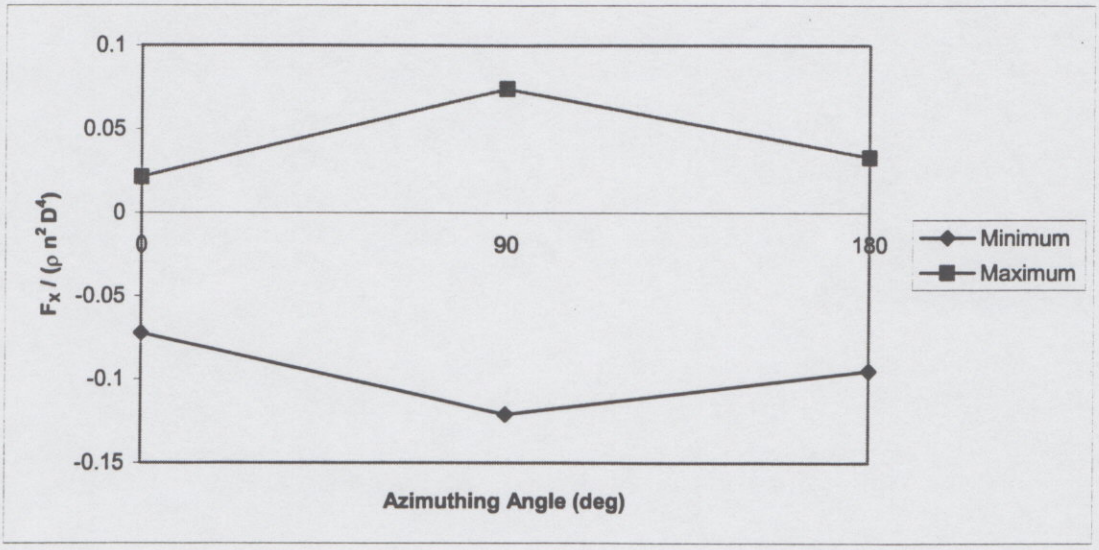

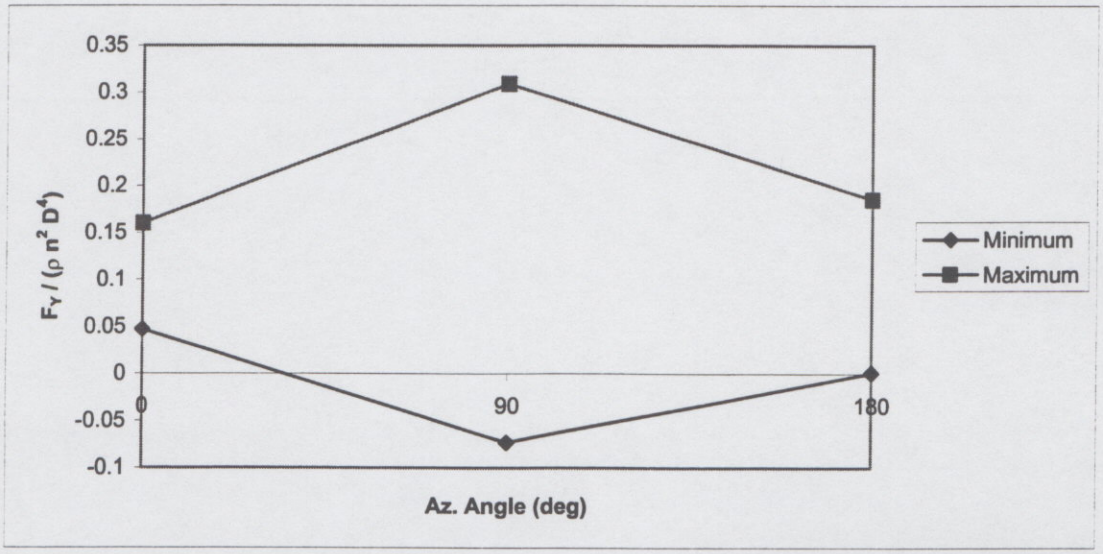

Fig. 9. – F_X and F_Y forces of forward dynamometer for clear water (J = 0.1)

5.2 In ice

Some of the ice tests results are presented in this section. These results are rather highlights of the preliminary experiments and intended to demonstrate the capabilities of the model designed. More detailed ice tank tests are underway.

The draft of the model stern was set at 6cm to help the ice sheet reach to the propeller. During the experiments, it was observed that the ice sheet broke along the longitudinal pre-cut lines. Then it was pulled beneath the model stern towards the propeller. At times, it was noticed that the ice sheet section would further brake into approximately 40 cm long panels across the width before reaching the propeller. This caused the ice reaching to the propeller in panels rather than as a continuous sheet, and somewhat irregularly. Regular checks of depth of cut were conducted to ensure the target depth of cut was achieved. The effects of this phenomenon may be noticeable in the records of the sensors. Fig. 10 shows a sample record for the global F_X force. Though the scales were different, a similar pattern was observed on the Fx force of the forward dynamometer as shown in Fig. 11.

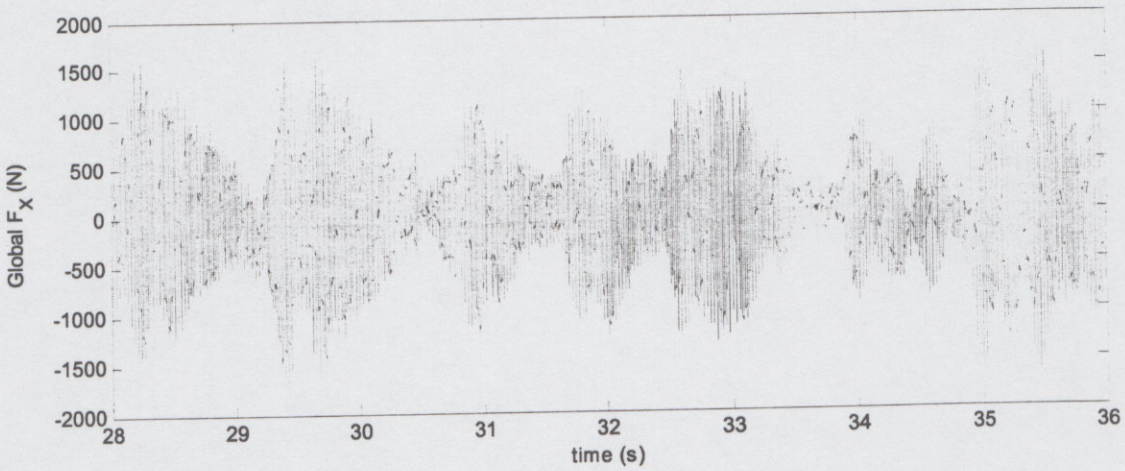

Fig. 10 – The effects of ice panels reaching to the propeller on global F_X force.

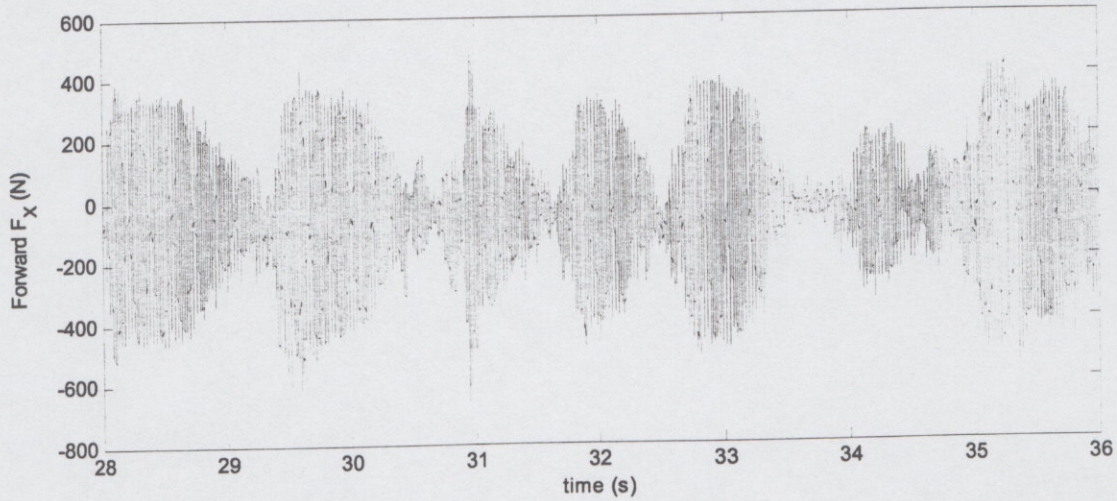

Fig. 11 – The effects of ice panels reaching to the propeller on F_X force of forward dynamometer.

Measuring the angular position of the blade, to which a six component dynamometer was attached, enabled a correlation between the loads on the bearings and the ice encounters. The zero position for the angle was set to be when the blade was down and perpendicular to the ice sheet. Using

different depths of cuts of each run, the angles at which the blade hit the ice sheet and exited the ice sheet were estimated. An example is given for the time series shown in Fig. 11. The time period selected is from 30s to 30.16s. In Fig. 12, the broken line represents the angular position of the blade. F_X force of the forward dynamometer is shown with a solid line. It is clear from the figure that in one cycle of the propeller, the forward bearing experienced a peak and a trough four times, which is equivalent to the number of blades. One can also estimate the corresponding angles to these peak values from the figure.

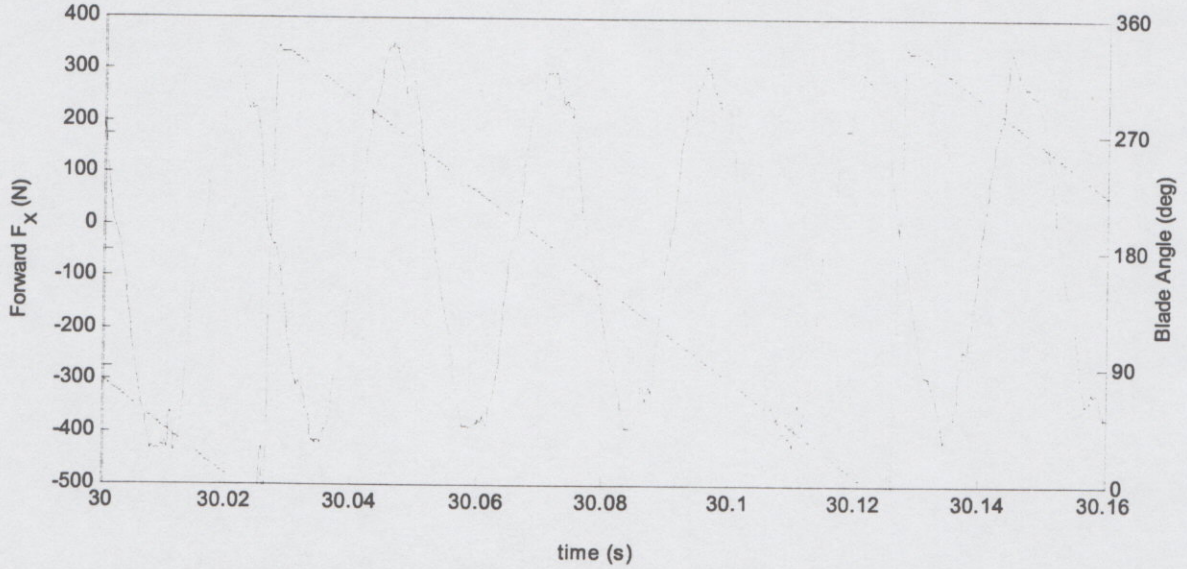

Fig. 12 – Cyclic loads on the propeller shaft bearings (broken line is blade angular position; solid line is F_X of forward dynamometer).

Assuming that during a test the depth of cut (maximum penetration into the ice) did not change and the angle where the blade hit the ice can be approximated using the tip of the blade, the entrance and exit angles to ice sheet can be estimated (
Fig. 13).

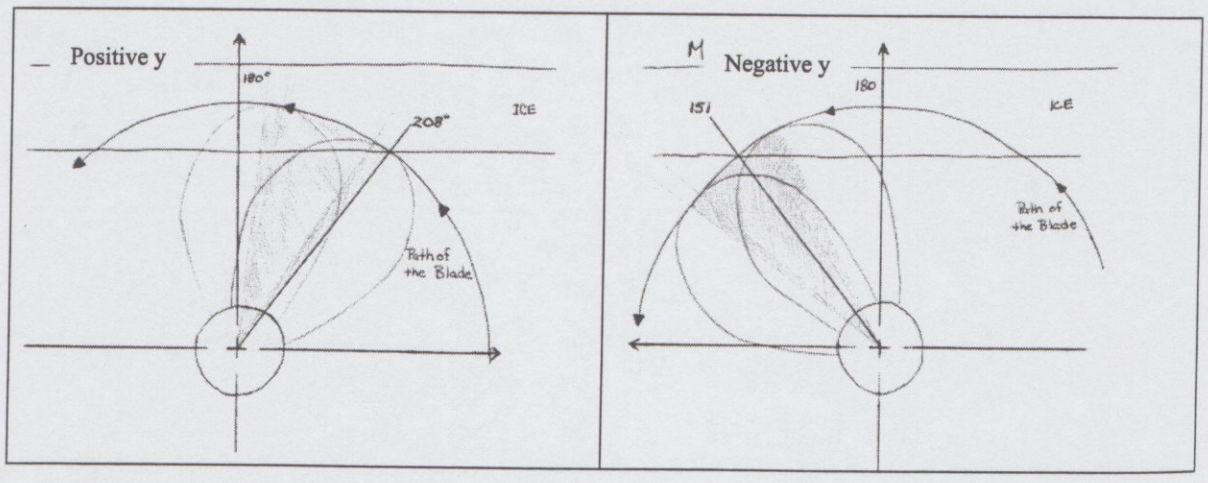

Fig. 13 - Sketch of the location of the maximum and minimum forces on the forward dynomometer

Based on these assumptions, the data obtained so far suggest that the maximum F_X forces on the forward dynamometer were observed as the blade entered and exited the ice sheet.

Using the global dynamometer readings, it was possible to calculate the total force in global X direction at different conditions. Given in Fig. 14 are the non-dimensional global F_X forces experienced at clear water and ice conditions. The test conditions are given in Table 1. This was a rather weak ice sheet. However, the target thickness was maintained. The ice effects in the figure are calculated as follows:

Regression line for *Ice effects* = (regression line for *In clear water*) – (regression line for *In ice*)

These regression lines are valid only for this ice condition. Additional tests are required to investigate the effects of varying ice sheet thickness and strength values.

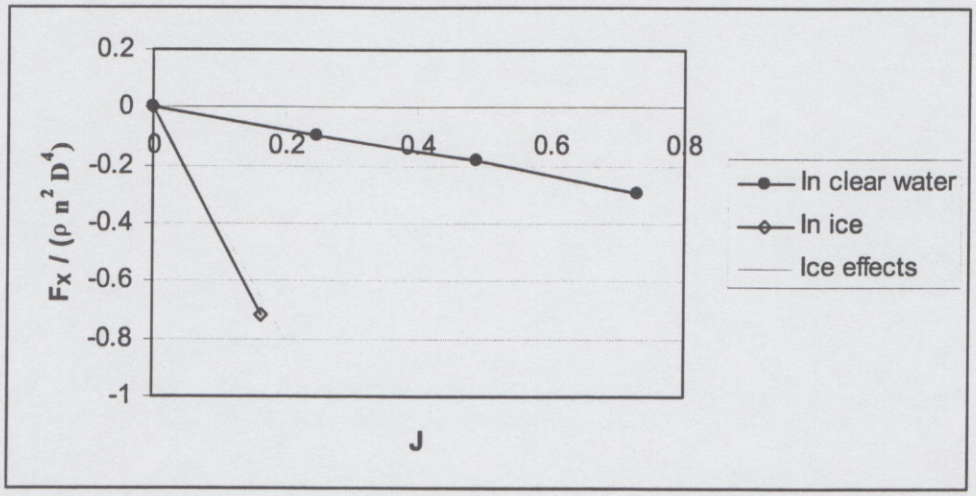

Fig. 14 – Non-dimensional global F_X force as a function of advance coefficient J. (Push mode, zero azimuthing angle)

Table 1- Average ice sheet properties

Azimuth angle (deg)	Density (kg/m^3)	Compressive Strength (kPa)	Flexural Strength (kPa)	Thickness (mm)
0	937	91	9	63

6. Conclusions

The preceding showed some of the results obtained from the preliminary tests done with the podded propulsor model designed and built at IOT. The aim was to demonstrate the capabilities of the experimental model developed rather than to draw general conclusions about the performance of podded propulsors in ice. In order to do that, additional tests are required. Some observations obtained from these preliminary tests are as follows:

- Due to the flow induced by the propeller, a side force on the model was experienced. This could be important to manoeuvering and directional stability of vessels outfitted with podded propulsors.
- Larger loads were experienced on the forward bearing dynamometer when the blades entered and exited the ice.
- Ice effects can be determined for different operating conditions.

Required further ice tank tests are scheduled in the near future.

7. Acknowledgements

The study on the podded propellers is a joint project between Transport Canada and the National Research Council of Canada. Furthermore, thanks are due to Memorial University's Technical Services Department for their help in the experimental work. Special thanks are extended to the members of the NRC- IOT for their assistance in various stages of this project.

8. References

1. Anonymous, (1995), "Azipods for last two Carnival liners from Masa-Yards", Naval Architect, November, p. 605.
2. Anonymous, (1997), "Hamlet joins the Helsingor-Helsingborg shuttle", Naval Architect, July/August, p. 20.
3. Anonymous, (1997) Twin-propeller pod with fins from Schottel, Naval Architect, July/August p. 31
4. Jones, S. J., (1987), "Ice Tank Test Procedures at the Institute for Marine Dynamics," Institute for Marine Dynamics Report No. LM-AVR-20
5. Timco, G.W., (1986), "EG/AD/S: A New Type of Model Ice for Refrigerated Towing Tanks," Cold Regions Science and Technology, Vol. 12, pp. 175-195